의학석사 학위논문

자성나노입자를 이용한 항암 열화학 병합치료의 유용성에 관한 연구

Study on the feasibility of antitumor thermochemotherapy using magnetic nanoparticle

2014년 8월

서울대학교 대학원

의과학과 의과학전공

전 민 정

자성나노입자를 이용한 항암 열화학 병합치료의 유용성에 관한 연구

지도교수 김 현 진

이 논문을 의학 석사 학위논문으로 제출함

2014 년 8 월

서울대학교 대학원

의과학과 의과학전공

전 민 정

전민정의 석사 학위논문을 인준함

2014 년 8 월

위 원 장 _____

부위원장 김 현진

위 원 _____

Study on the feasibility of antitumor thermochemotherapy using magnetic nanoparticle

by

Min Jeong Jeon

A Thesis Submitted to the Department of Biomedical science in Partial Fulfilment of the Requirements for the Degree of Master of Biomedical science at the Seoul National University College of Medicine

August, 2014

Approved by thesis committee:

Professor _____ Chairman

Professor Hyeonjin Kim. Vice Chairman

Professor _____

Abstract

The aim of this study was to evaluate the efficacy of intratumoral delivery of ferucarbotran, a clinically approved magnetic nanoparticles (MNPs), conjugated with doxorubicin to simultaneously induce magnetic hyperthermia and chemotherapeutic effect in a hepatocellular carcinoma (HCC) model. Human HCC cells expressing luciferase were subcutaneously implanted into the right flank of 6-week–old BALB/c-nu mice (n=19). When the tumor diameter reached 7-8 mm, the animals were divided into four groups according to the injected agents: group A (normal saline, n=4), group B (doxorubicin, n=5), group C (MNP, n=5), and group D (MNP/doxorubicin complex, n=5). Animals were placed in the center of an AC coil to generate an alternating magnetic field (AMF) to receive magnetic hyperthermia, and intratumoral temperature changes were measured using a thermo-sensor. Bioluminescence imagings (BLIs) were performed before treatment and at 3, 7, and 14 days after treatment to measure the biological activities of the tumors during the follow-up period. The relative signal intensity (RSI) of each tumor was calculated by dividing the BLI signal at each time point by the initial value measured before treatment. After the completion of follow-up, all the animals were euthanized to assess the apoptosis rates of tumors on pathologic examination. The rise in temperature in the tumors was 1.88±0.21 °C in group A, 0.96±1.05 °C in B, 7.93±1.99 °C in C, and 8.95±1.31 °C in D. The RSI of the tumors at day 14 post-treatment was significantly lower in group D (0.31±0.20) than in in group A (2.23±1.14), B (0.94±0.47), and C (1.02±0.21). The apoptosis rates of the tumors as determined by histopathological analyses were 11.52±3.10% in group A, 23.0±7.68% in B, 25.4±3.36% in C, and 39.0±13.2% in D, respectively. The intratumoral injection of clinically approved MNPs conjugated with

doxorubicin exhibits an improved therapeutic benefit compared with the injection of doxorubicin or MNP alone when the complex is injected into HCC tissues exposed to AMF for magnetic hyperthermia. This strategy of combining doxorubicin and MNP-induced magnetic hyperthermia exhibits a synergic effect on inhibiting tumor growth in an HCC model.

Keywords : hepatocellular carcinoma (HCC), magnetic nanoparticle (MNP), magnetic hyperthermia, drug delivery system (DDS), bioluminescence imaging (BLI)

Student number : 2012-23674

CONTENTS

Page

LIST OF TABLE

LIST OF FIGURES

LIST OF ABBREVIATION

MNP, magnetic nanoparticle

HCC, hepatocellular carcinoma

AMF, alternating magnetic field

BLI, Bioluminescence imaging

RSI, Relative signal intensity

DDS, Drug delivery system

Introduction

Hepatocellular carcinoma (HCC) remains the fifth most common cancer as well as the third leading cause of cancer mortality worldwide (El-Serag HB, Rudolph L, 2007). Current therapeutic options, including surgical resection, radiotherapy, and chemotherapy, have been unsatisfactory in most patients. Although surgical resection has been recognized the most effective treatment for HCC, its efficacy is limited to the minority of patients who have early stage disease. Patients with underlying liver disease, unsuitability for resection, or little organ availability for transplantation are not candidates for surgery (Schwartz M et al., 2007).

Hyperthermia is a very promising cancer treatment based on the hypothesis that cancerous cells are more sensitive to an increase in the tissue temperature than normal cells (Hegyi Gabriella et al., 2013). In recent years, various hyperthermic ablation therapies such as radiofrequency ablation, microwave ablation, and high intensity focused ultrasound have been widely introduced especially for liver cancer. Another strategy for heat induction in tumor is magnetic hyperthermia. When exposed to a high-frequency magnetic field, magnetic nanoparticles (MNPs) generate heat through the oscillation of their magnetic moment due to Neel and Brownian relaxations (Jordan A et al.,

2009). Direct injection of MNPs into solid tumors, followed by exposure of tumors to an alternating magnetic field (AMF), has been shown to induce controlled heating at the target tumors, which leads to tumor regression (Ito A et al., 2003). After exposure of tumor-bearing organs to AMF, the induced heat that raises the tissue temperature to approximately 41–47°C is known to alter the function of many structural and enzymatic proteins within cells, which in turn arrests cell growth and differentiation and eventually induces apoptosis (Wust P et al., 2006, Hilger I et al., 2000). This particle-induced magnetic heating can be controlled by accurate and localized delivery of the MNPs to the target lesions, and has been under several clinical trials (Thiesen B and Jordan A, 2008). Additionally, MNPs have been investigated as drug delivery systems to improve the efficacy of drugs. The loading of drugs to MNPs can be achieved either by conjugating the therapeutic agents onto the surface of the MNPs or by co-encapsulating the drug molecules along with MNPs within the coating material envelope (Wahajuddin and Arora S, 2012). Once at the target site, MNPs can stimulate drug uptake within cancer cells by locally providing high extracellular concentrations of the drug or by direct action on the permeability of cell membranes (Hong S et al., 2006). Most of MNPs are not approved for use in humans because their safety and toxicity have not been clearly documented. However, ferucarbotran (Resovist; Bayer

Schering Pharma AG, Leverkusen, Germany) is a clinically-approved superparamagnetic iron oxide nanoparticle that has been developed for contrast-enhanced MRI of the liver (Reimer P and Balzer T, 2003).

Local hyperthermia of tumor tissue in conjunction with chemotherapy has been demonstrated to significantly enhance antitumor efficacy (de Smet M et al., 2013). Here, we designed a complex made with both Resovist, an MNP approved for clinical use in humans, and doxorubicin to combine the magnetic control of heating and drug delivery into one treatment. We expected that this complex would enhance the synergistic efficacy and yield substantial promise for a highly efficient therapeutic strategy in HCC. The in vivo antitumor effect was evaluated by bioluminescence imaging (BLI), which measures the luciferase-expressing tumor cells' activity, throughout the follow-up period.

Materials and Methods

Preparation of the Resovist/doxorubicin complex

Resovist was loaded with doxorubicin through ionic interactions between anionically charged carboxy dextran coating layer of Resovist and positively charged amino groups of doxorubicin. Predetermined amount of doxorubicin (0.2 mg, Adriamycin; Ildong Pharmaceutical, Seoul, Republic of Korea) was dissolved in 4 mL deionized water, and the aqueous solution was transferred to a 250 mL round-bottom flask. Diluted (1.38 Fe mg/mL) Resovist in 4 mL deionized water was added dropwise using a syringe pump at a rate of 0.1 mL/min, and the reaction mixture was vigorously stirred for 8 hours. Loading efficiency of doxorubicin was 100 % and ultraviolet-visible spectroscopy at 480 nm confirmed that there was not any doxorubicin left in the aqueous solution. The Resovist/ doxorubicin complex was obtained as a solid after freeze-drying and the diameter of the complex before and after the freeze-drying was not so different based on DLS data. The concentration of doxorubicin in the complex was adjusted to 1mg/ml.

The in vitro release test of the Resovist/doxorubicin complex

The release profile of doxorubicin from the complex was evaluated by the

dialysis method. Two milliliters aqueous solution of the complex conjugated to doxorubicin (2 mg) was transferred into a dialysis membrane with a molecular weight cutoff of 1 K and dialyzed against deionized water (20 mL). The temperature of the medium was changed to either 37°C or 60°C at a predetermined time, and an aliquot was sampled at 1, 2, 3, 4, 5, 6, 18, 42 and 66 h. The amount of released doxorubicin was measured by ultraviolet-visible spectroscopy at 480 nm.

Measurement of the relaxivity of the Resovist/doxorubicin complex

To test whether the conjugation process would affect the MR imaging of Resovist, we measured the MR relaxivity of the Resovist/doxorubicin complex, which was compared with that of Resovist. The particles were serially diluted from a concentration of 0.15 mM in an agarose phantom designed for relaxivity measurements, which was done using a 3-T MR scanner (Tim Trio; Siemens Healthcare, Erlangen, Germany). Fast spin echo T2-weighted MR images of the phantom were acquired using the following parameters: relaxation time = 5000 ms, echo times = 16, 32, 48, 64, 20, 40, 60, 80, 50, or 100 ms, flip angle = 180, ETL = 18 fields of view, FOV =77x110 mm2, matrix = 256x117, slice thickness / gap = 1.4 mm / 1.8 mm, and NEX = 1.

Preparation of the animal model

Hep3B, a human HCC cell-line, was transduced with a retroviral vector containing the firefly luciferase (luc) reporter gene, and a highly expressing reporter clone was isolated to establish Hep3B+luc cells. Hep3B+luc cells were cultured in Dulbecco's modified Eagle's medium (DMEM; Welgene, Seoul, Korea) supplemented with 10% (v/v) heat-inactivated fetal bovine serum (GIBCO, Seoul, Korea). All animal procedures were performed according to the Seoul National University Institutional Animal Care and Use Committee-approved protocol (SNUH-IACUC #12-0015). Male BALB/c-nude mice (n=19), aged 6 weeks and weighing 20–25 g, were used for this study. Hep3B+luc cells were suspended at $1x10^6$ cells/0.1 ml in serum-free DMEM and subcutaneously injected into the right flanks of the animals. Two weeks after tumor implantation, when the tumor diameter reached approximately 7-8 mm in diameter, the animals were evenly divided into 4 groups according to the injected agents: group A (n=4) injected with normal saline, group B (n=5) with doxorubicin (4 mg/kg), group C (n=5) with Resovist (Fe 111.6 mg/kg), and group D (n=5) with the Resovist/doxorubicin complex (Fe 111.6 mg/kg, doxorubicin 4 mg/kg). All therapeutic agents were dissolved in the same volume of saline (0.1 ml) and injected directly into the

core of tumors.

Magnetic hyperthermia

The animals were fully anesthetized by intraperitoneal administration of 12 mg/kg tiletamine-zolazepam (Zoletil 50; Virbac, Carros, France) and 0.75 mg/kg xylazine hydrochloride (Rompun; Bayer, Seoul, South Korea). The animals were then placed in the center of AC coil to generate AMF (Figure 1). An original device was connected to the coil (width 30 cm, length 30 cm) and cooling unit, which was cooled continuously by flowing water by the unit (Recirculating coolers HX-45H; Jeiotech, Daejeon-si, Korea). A high-frequency generator worked at a current of 155 Oe at a frequency of 100 kHz for magnetic hyperthermia. A 20-gauge venipuncture catheter (BD Angiocath Plus with intravenous catheter; Becton Dickinson Korea, Gumi-si, Korea) was inserted into each tumor so that an electronic thermometer (Luxtron m3300 Biomedical Lab Kit Fluoroptic Thermometer; LumaSense Technologies, Santa Clara, CA) could be passed through the catheter to measure the core temperature of the tumor during the procedure. To evaluate the selectivity of heating during the hyperthermia treatment, rectal temperatures were simultaneously measured in a same manner as described above.

Bioluminescence imaging for the in vivo evaluation of therapeutic responses

Bioluminescence imaging (BLI) was performed using the IVIS lumina II (PerkinElmer, Waltham, MA). Mice were anesthetized with 1% isoflurane (Ifran, Hana Pharm. Co, Seoul, Korea) in room air. D-luciferin (Caliper Life Sciences, Hopkinton, MA) dissolved in PBS (1.5 mg luciferin/100 ul PBS) was injected intraperitoneally at a dose of 150 mg luciferin/kg, and serial images were acquired with an exposure time of 30 sec, an f/stop of 1, and pixel binning at 8 over 20 minutes to determine the peak bioluminescence. Subsequently, regions of interest (ROIs) of equal size were drawn within the tumor to measure average radiance (expressed as photons/s/cm2/sr). The BLIs were performed just prior to treatment to obtain the baseline value and at 3, 7 and 14 days after treatment. By using Living Image® 4.2 software (Caliper Life Sciences, Hopkinton, MA), we measured the peak total tumor bioluminescent signal through standardized ROIs. To ensure longitudinal comparability of the serial measurements, we calculated the relative signal intensities (RSIs) by normalizing each measured peak total tumor bioluminescent signal in a mouse with the signal at baseline as follows: [RSI at a time-point = (peak signal intensity at a time-point /peak signal intensity at baseline)] (Kelsey L et al., 2011).

Histopathological evaluations

All animals were euthanized at day 14 after treatment. The extracted tumors were perfused with PBS, fixed in 4% paraformaldehyde solution, and embedded in paraffin. The tumors were sectioned at a thickness of 4 μm at the largest tumor area. Hematoxylin and eosin (H&E) staining was performed for a general inspection of the pathologic specimens. Prussian blue staining was added to visualize the injected iron particle distribution within the tumor tissues. To evaluate the extent of tumor apoptosis for validating in vivo BLI results, a terminal deoxynucleotidyl transferase dUTP nick end labeling (TUNEL) assay was performed with a commercial kit (Roche, Mannheim, Germany). TUNEL staining is a method to stain cells exhibiting apoptotic or non-apoptotic DNA damage (i.e., DNA fragmentation), such as necrotic cell death (Jordan A et al., 2009, Li SD and Huang L, 2009). The percent area of apoptosis was calculated using NIH Image J software (NIH, Bethesda, MD). After drawing a free-hand ROI to completely cover the tumor, the number of pixels in the tumor area was counted. Within the selected tumor area, the number of pixels corresponding to the apoptosis area stained with TUNEL was also counted. The percent area of apoptosis (%) was calculated by dividing the area of the TUNEL-stained area (pixels) by the area of the total

tumor (pixels).

Doxorubicin fluorescence microscopy

Fourteen days after treatment, some of the extracted tumor tissues were immediately cryosectioned at a thickness of 6 μm in the largest tumor and stored at -70°C. After washing the tissues, the cover slips were mounted onto glass slides using mounting medium (Faramount aqueous mounting medium; Dako, Carpinteria, CA). On the slides, the distribution of doxorubicin over the tumor area was observed under a fluorescence microscope (Leica DM5500B, Leica, Wetzlar, Germany) using excitation and emission wavelengths of 520 and 580 nm, respectively. The fluorescence images were acquired using the following parameters: magnification=200x, BF:EX14 Gain 1.1 Intensity 1 gamma 45, and FLU: EX 656 Gain 4 Intensity 5 gamma 20.

Statistical analyses

All data are expressed as means ± standard deviation (SD), and the data processing and analysis were performed using SPSS version 16.0 (SPSS, Inc., an IBM Company, Chicago, IL). The nonparametric analysis was conducted by the Mann-Whitney test to compare the temperature changes in tumors, BLIs values, and apoptosis rates between the experimental groups. A p-value

of less than 0.05 was considered statistically significant.

Results

The size and relaxivity of the Resovist/doxorubicin complex

The size of Resovist measured by dynamic light scattering was 70.3±31.5 nm and increased to 88.4±39.5 nm when doxorubicin was conjugated on the surface (Fig. 2). The amount of doxorubicin was adjusted to be 2 mg/mL at the final administration for our study. Because the amount of doxorubicin was not a maximized value, the loading efficiency was 100%. The Resovist/doxorubicin complex was freeze-dried and stored as a solid. Redispersion of the complex by vortexing and/or sonication resulted in a similar size distribution reproducibly without any difficulties. When measuring the T2 relaxivities of the particles, the r2 values of Resovist and the Resovist/doxorubicin complex were 295.0 s−1mM−1 and 265.7 s−1 mM−1, respectively (Fig. 3).

In vitro release from the Resovist/doxorubicin complex

Figure 4 summarizes the release pattern of doxorubicin from the complex. The driving force for the doxorubicin conjugation is an ionic interaction, which is known to weaken as the temperature increases. The release test was performed at two different temperature, 37°C and 60°C, with a predetermined

time profile to mimic the condition of hyperthermal therapy. As expected, sustained release of doxorubicin was observed at 37°C, whereas the release was accelerated at the elevated temperature.

Tumor temperature measurement

The tumor temperature in group C and D rapidly increased to approximately 42°C within 5 minutes and then remained stable for 20 minutes, whereas in group A and B did not increased significantly (Fig. 5A). The average values of tumor temperature change 25 minutes after initiation of hyperthermia were 1.88±0.21°C in group A, 0.96±1.05°C in group B, 7.93±1.99°C in group C, and 8.95±1.31°C in group D (Fig. 5B). Group C and D exhibited a significantly higher temperature in the tumors than group A or B ($p < 0.05$). The exact p-values obtained from comparisons between groups are summarized in table 1. The rectal temperatures in all groups remained stable near the baseline values during the treatment.

Bioluminescence imaging findings

In group A receiving normal saline for control, the RSI of BLI increased continuously over the follow-up period reflecting active tumor growth (2.23±1.14). In group B, the RSI of BLI slightly decreased gradually until day

14 post-treatment (0.94±0.47), which suggests that the cytotoxic effect of doxorubicin works on the tumor slowly (Fig. 6A, B). In group C, the RSI of the BLI rapidly dropped 3 days after treatment and rebounded to near-baseline value at day 14 post-treatment(1.02±0.21), suggesting complete recovery of tumoral activities at the later stage of treatment (Fig. 6A, B). However, the RSI of BLI in group D dropped 3 days after treatment as in group C and exhibited minimal recovery until day 14 post-treatment (0.31±0.20) (Fig. 6A, B).The Mann-Whitney test performed for the BLI values at day 14 post-treatment revealed that the RSI of BLI in group D was significantly lower than the other groups (all p-values < 0.05) (Fig. 6C). The exact p-values obtained between groups are summarized in table 1. No mouse exhibited signs of debilitation in any of the groups through the follow-up period.

Histopathological findings

TUNEL assay of the tumor tissues obtained at day 14 by revealed that the apoptosis/necrosis rate in group D was higher (39.0±13.2) than group A (11.52±3.10), B (25.4±3.36), and C (23.0±7.68) (Fig. 7). Therefore, the Resovist/doxorubicin complex showed significantly more cell death than doxorubicin or Resovist monotherapy (all p-values < 0.05). The exact p-values obtained between groups are summarized in table 1. Prussian blue

staining of the consecutive section demonstrated multiple iron deposits within the tumor tissues in groups C and D (Fig. 8).

Doxorubicin fluorescence microscopic findings

On fluorescence microscopic examination, group D exhibited higher fluorescence intensity from doxorubicin in the tumor tissues, which significantly overlapped the area with the iron particles. By contrast, group B exhibited minimal fluorescence from doxorubicin (Fig. 9). This result suggests that the Resovist/doxorubicin complex could release doxorubicin into the tumor tissues in a controlled manner for a longer period than free doxorubicin and allowed persistent drug accumulation.

Table 1. Comparisons of the temperature changes in tumor, RSIs of BLI at day 14 post-treatment, and apoptosis rates between groups. Each number in the table indicates a p-value obtained by Mann-Whitney test (*p < 0.01, **p < 0.05).

	Group B vs. C	Group B vs. D	Group C vs. D
Temperature Changes	0.009*	0.009*	0.465
RSIs of BLI	0.834	0.047**	0.009*
Apoptosis Rates	0.675	0.028**	0.008*

A

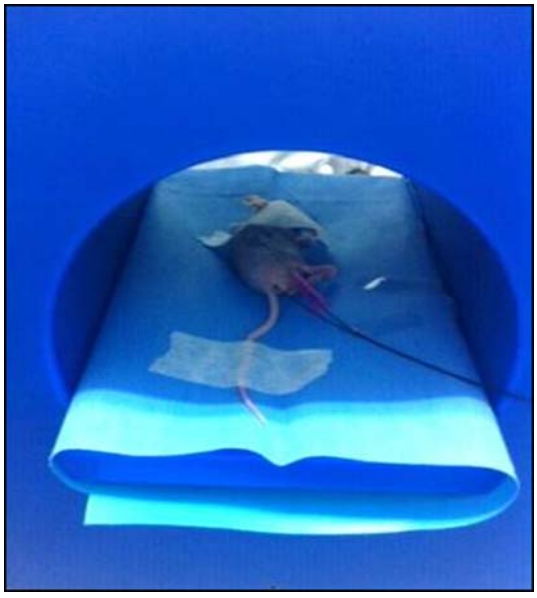

B

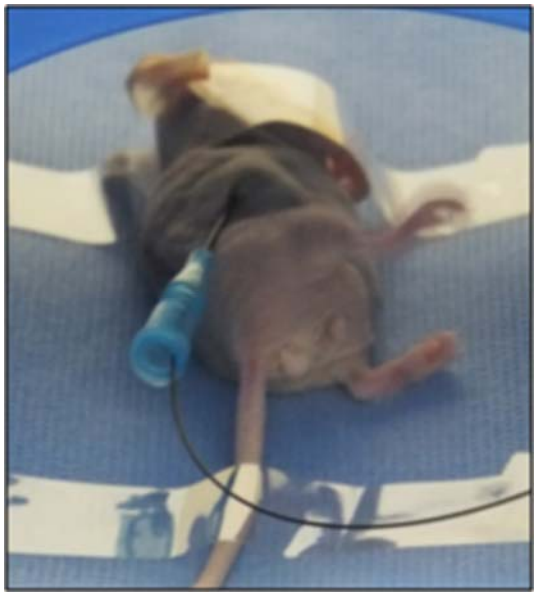

Figure 1. Photograph of hyperthermia treatment.

(A) A tumor-bearing mouse is placed in the center of hyperthermia device generating AMF.

(B) A thermo-sensor is inserted into tumor by way of a venipuncture catheter to measure temperature changes during the treatment.

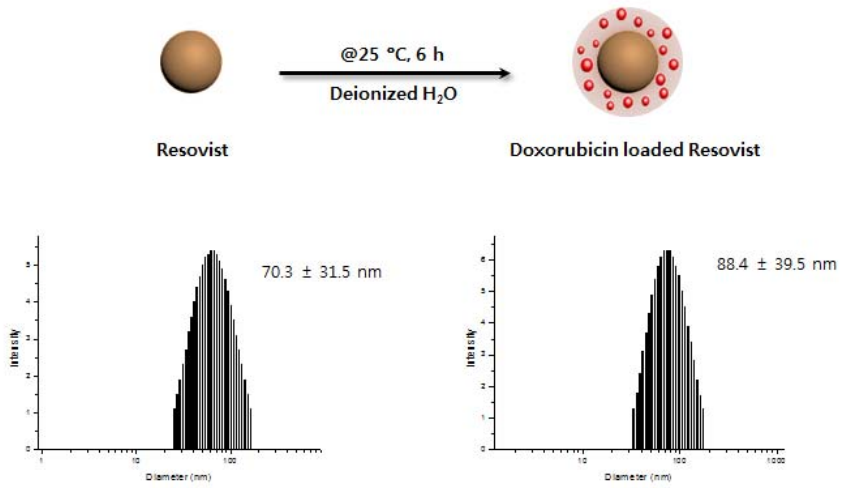

Figure 2. Preparation and characterization of Resovist-doxorubicin complex.

A

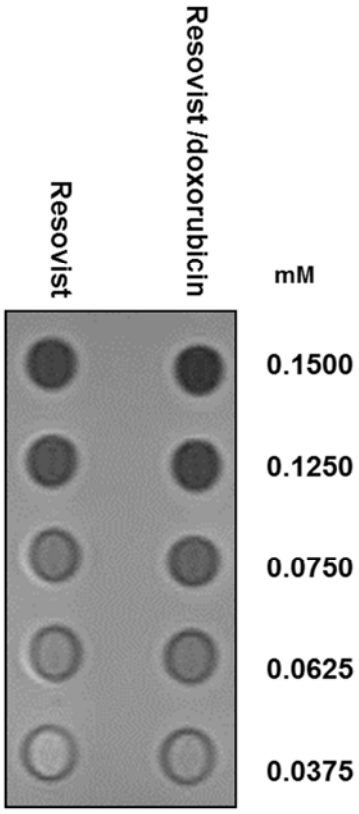
Resovist
Resovist /doxorubicin
mM
0.1500
0.1250
0.0750
0.0625
0.0375

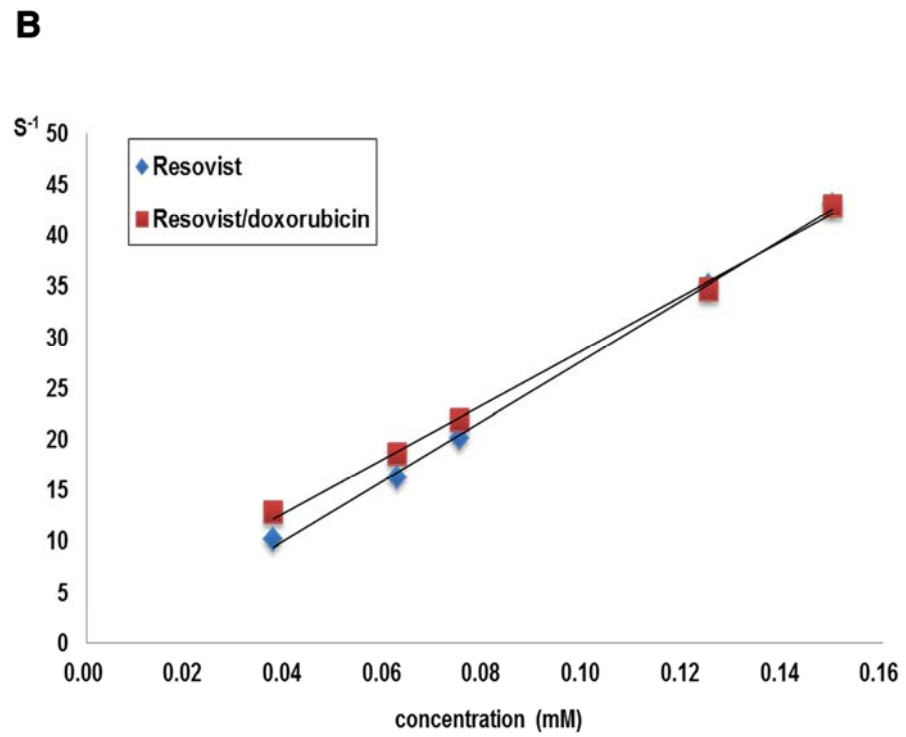

Figure 3. Measurement of MR relaxivities.

(A) T2-weighted MR image of the phantom for relaxivity measurement.

(B) Plot of the inverse transverse relaxation times (1/T2) vs. Fe concentration.

The slopes indicate the specific relaxivity value (r2).

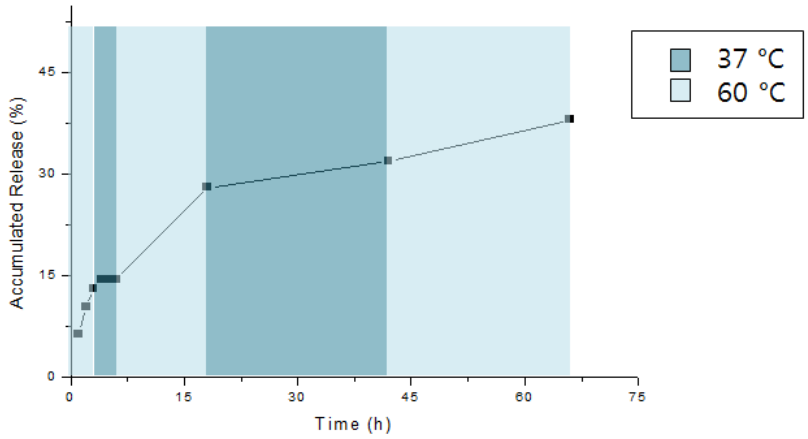

Figure 4. The in vitro release pattern of doxorubicin from the Resovist-doxorubicin complex..

A

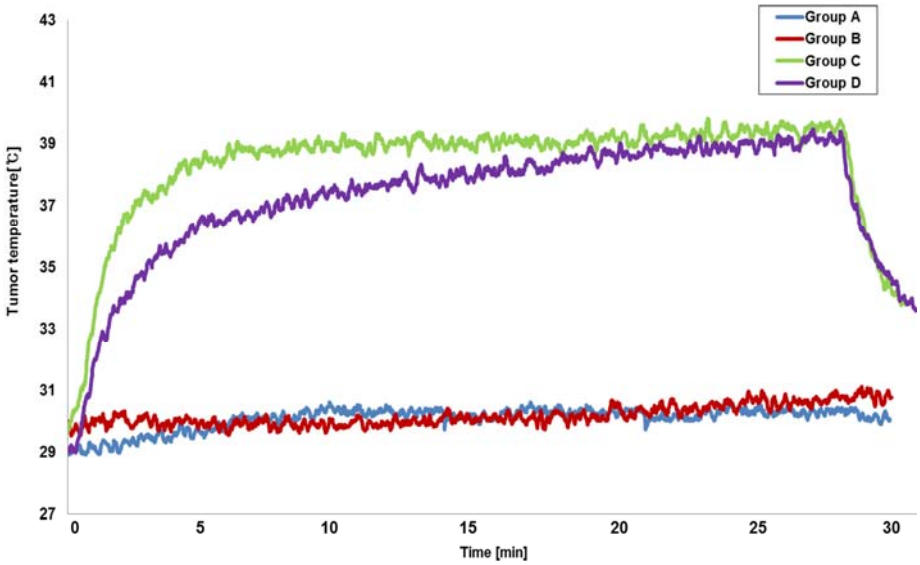
Group A
Group B
Group C
Group D
Tumor temperature[℃]
43
41
39
37
35
33
31
29
27
0
5
10
15
20
25
30
Time [min]

B

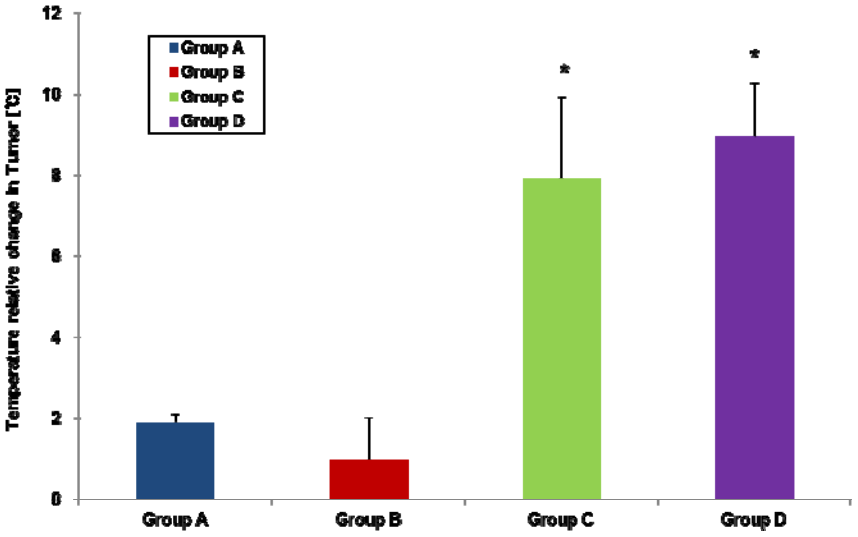
Group A
Group B
Group C
Group D
Temperature relative change in Tumor [℃]
12
10
8
6
4
2
0
*
*
Group A
Group B
Group C
Group D

Figure 5. The temperature changes of the tumors.

(A) Plot of the temperature change curve during heating versus time (blue: group A, red: group B, green: group C, purple: group D).

(B) The mean temperature changes of the tumors (t/t0) during treatment. The error bars represent the standard deviations(*p<0.05, compared to group A).

A

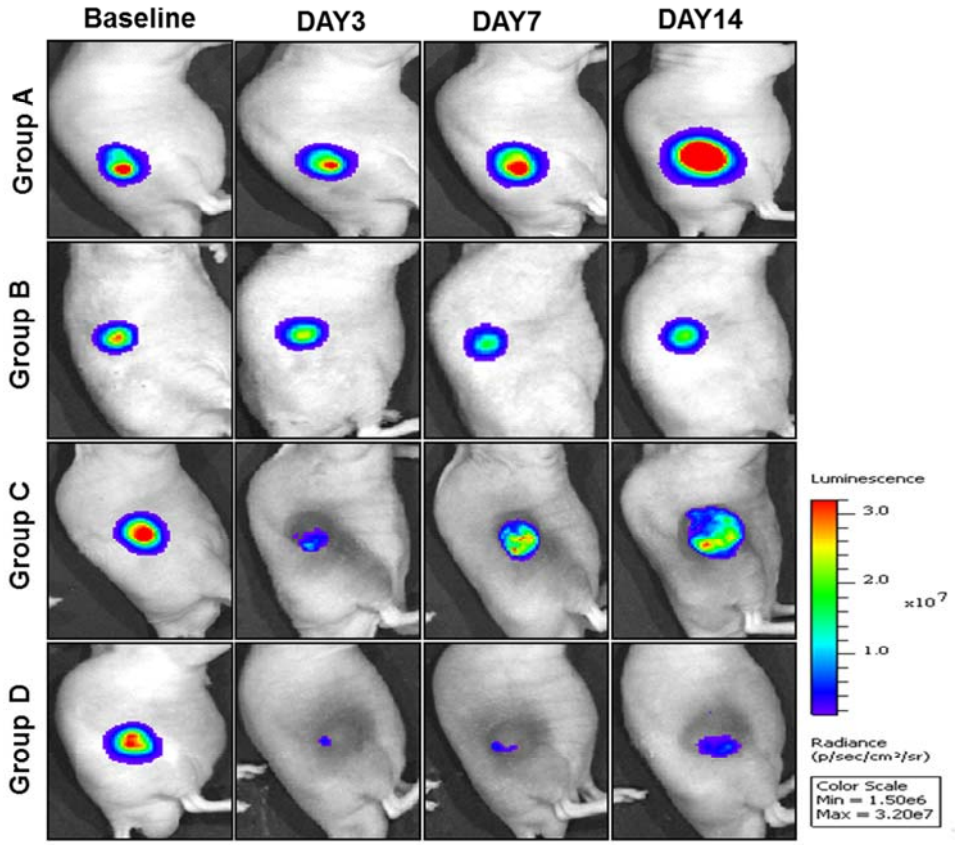
Baseline
DAY3
DAY7
DAY14
Group A
Group B
Group C
Group D
Luminescence
3.0
2.0
x10^7
1.0
Radiance
(p/sec/cm²/sr)
Color Scale
Min = 1.50e6
Max = 3.20e7

B

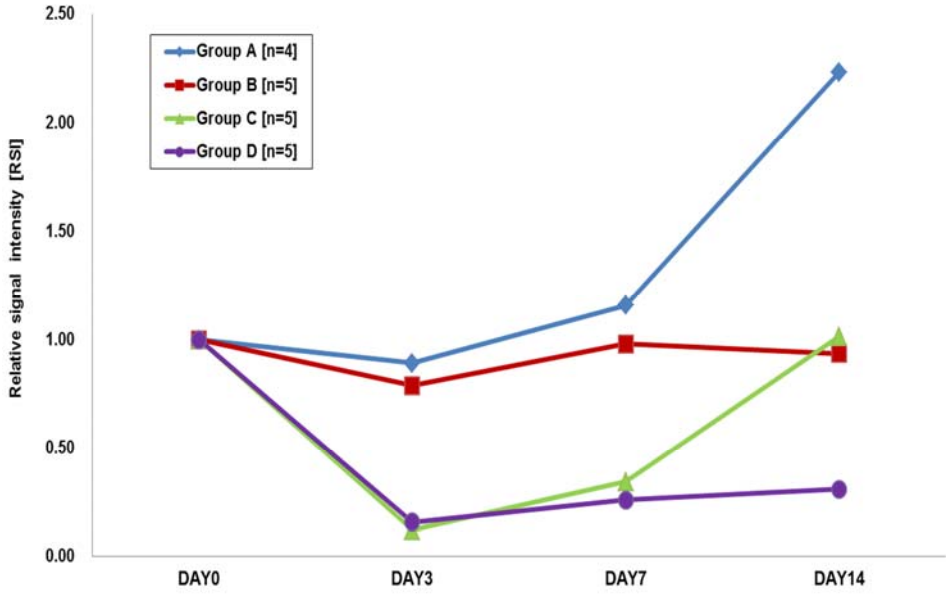
Group A [n=4]
Group B [n=5]
Group C [n=5]
Group D [n=5]
Relative signal intensity [RSI]
2.50
2.00
1.50
1.00
0.50
0.00
DAY0
DAY3
DAY7
DAY14

C

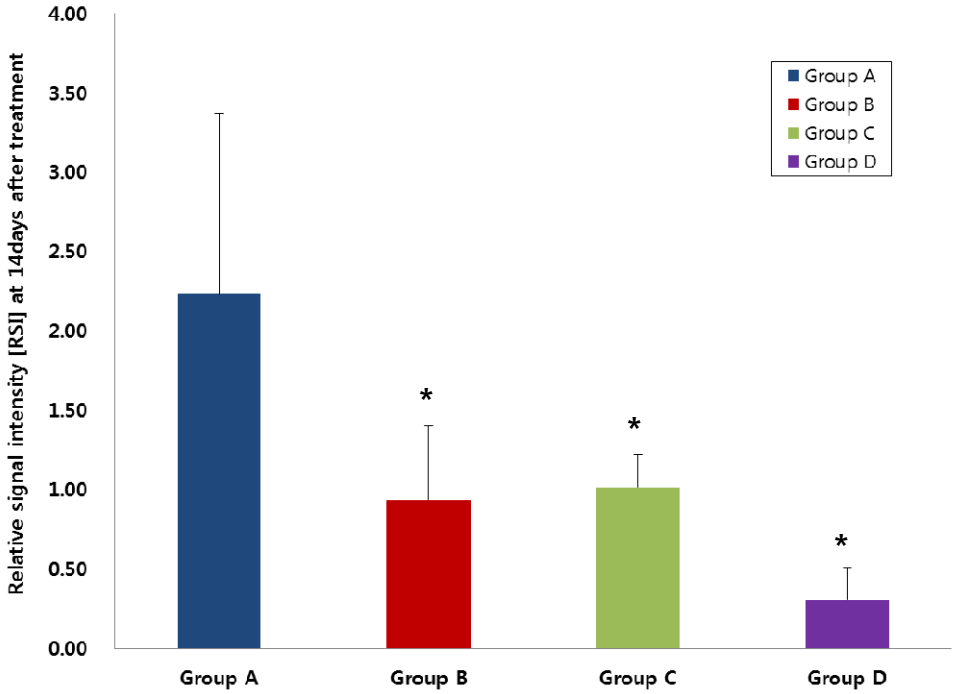
Relative signal intensity [RSI] at 14days after treatment
4.00
3.50
3.00
2.50
2.00
1.50
1.00
0.50
0.00
Group A
Group B
Group C
Group D
*
*
*

Figure 6. Bioluminescence imaging (BLI).

(A) Representative BLI obtained in each group by the IVIS lumina II (PerkinElmer, Waltham, MA).

(B) Relative signal intensity [RSI] of BLI over the follow-up period.

(C) A graph demonstrated the relative signal intensity [RSI] of BLI at 14 days after treatment. (*p<0.05, compared to group A).

A

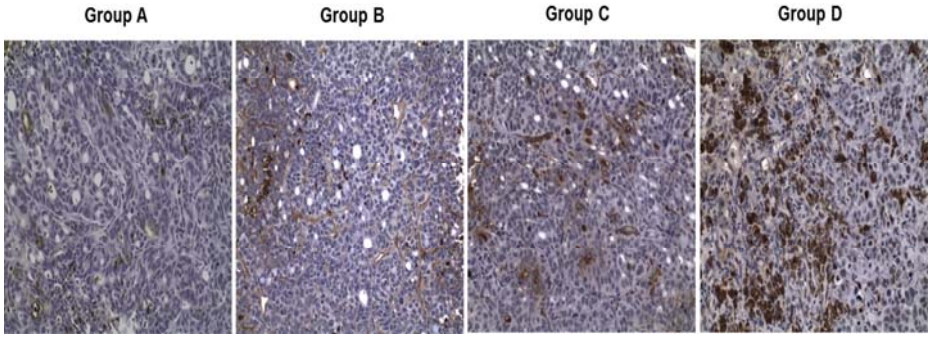
Group A
Group B
Group C
Group D

B

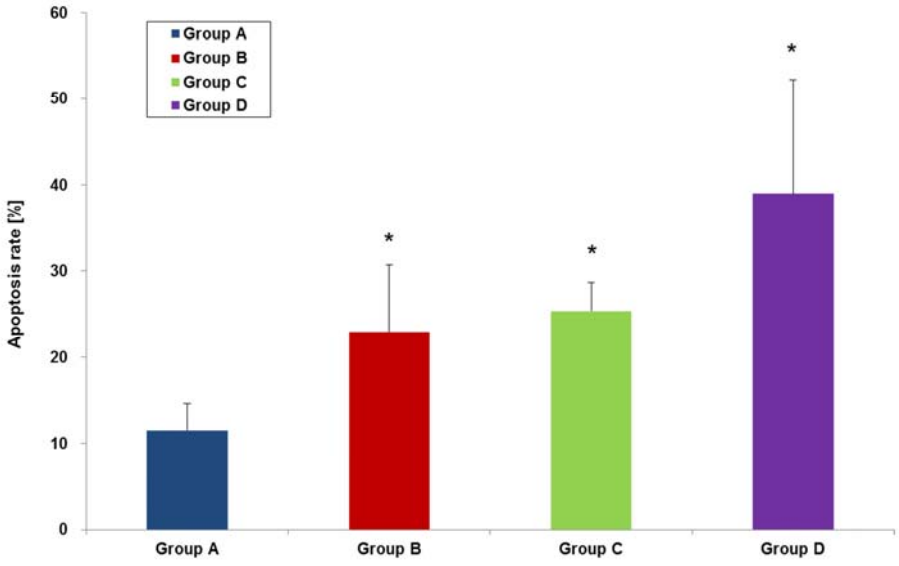
Group A
Group B
Group C
Group D
Apoptosis rate [%]
60
50
40
30
20
10
0
*
*
*
Group A
Group B
Group C
Group D

Figure 7. Terminal deoxynucleotidyl transferase-mediated nick end labeling (TUNEL) assays to measure apoptotic cell death by light microscopy.

(A) TUNEL-positive (brown color) cells with apoptotic morphology were observed in all groups (x200).

(B) A graph demonstrating the apoptosis/necrosis rates in all groups by image J software (*p<0.05, compared to group A).

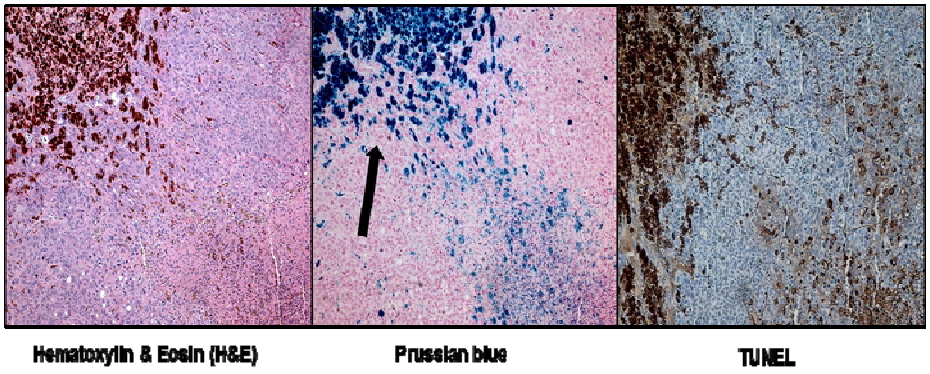

Figure 8. Histological analysis of the tumor tissues by using a light microscopy.

Hematoxylin and eosin staining(left), Prussian blue staining(middle), and TUNEL staining(right) of the tumor treated with Resovist/doxorubicin complex (x100). There is a well described dox-MNPs (arrow).

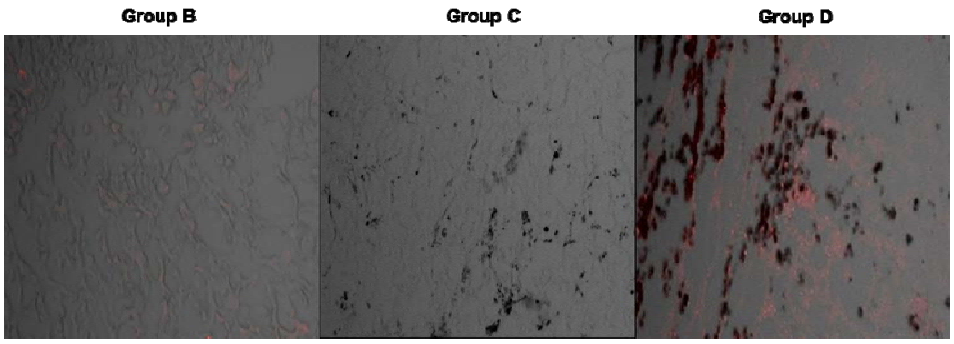

Figure 9. Fluorescence microscopy images

Representative fluorescence images of group B (left), group C (middle), and group D (right). Group D shows higher doxorubicin fluorescence signals than the other two groups.

Discussion

MNPs have gained considerable interest for biomedical applications over the past two decades (Cole AJ et al., 2011). Although this excitement has been driven mostly by the success of MNPs as T2 MR contrast agents (Weissleder R et al, 1990), the recent investigative trend has turned toward therapy with respect to cancer. The key properties of MNPs for cancer include drug delivery, magnetic hyperthermia, and MR imaging. Thus, MNPs contribute both diagnostic and therapeutic accomplishments in a single system.

Drug delivery systems are required to ensure that the drug is properly delivered to target, and nanoparticle-based drug delivery systems have been developed as potential drug carriers for decades. Because the large surface-to-volume ratio of MNPs, like other nano-carriers, enables a high loading of various functional ligands on a single platform, marked attention has been paid to their use as drug delivery vehicles. In our study, the loading efficiency of doxorubicin was 100%. The ultraviolet-visible spectroscopy at 480 nm confirmed that there were not any doxorubicin left in the aqueous solution, which led to a conclusion that washing step to remove unbound doxorubicin was not required. MNP coatings provide anchor points to which drug molecules can be coupled and have incorporated traditional small molecules

such as doxorubicin for cancer therapy (Veiseh O et al, 2010), as in our study. Resovist is coated with carboxydextran, to which doxorubicin was linked via ionic complexation by dropping synthesis with an average size of less than 100 nm in our study (Fig. 2). When Resovist/doxorubicin complex reached tumor tissues after intratumoral injection, the complex was able to carry higher concentrations and exhibited prolonged release of doxorubicin in the tumor tissues as measured by fluorescence microscopy (Fig. 9).

Magnetic hyperthermia can be used to selectively kill tumor cells via increases in tissue temperature (Jordan A et al., 2009). When MNPs accumulating at the tumor site are exposed to AMF, MNPs absorb this energy and convert it into heat owing to the relaxation of the rotating magnetic moments induced by the AC field. Tumors are usually heated to the temperature range of 41–47°C, and cancer tissues exhibit higher heat sensitivity than normal tissues (Purushotham S and Ramanujan RV, 2010). It also has been believed that the drug delivery to target could be increased by hyperthermia through its effects on convection and diffusion in tissues, increasing cell uptake of the drug, tumor blood flow and vascular permeability (Facy O et al., 2011). In our study, Resovist or the Resovist/doxorubicin complex also induced temperature increases to approximately 41°C (Fig. 5A). Although magnetic hyperthermia is a promising cancer therapy, the risk of

local overheating (and thus damage to normal tissues) remains the major concern, as in other clinical hyperthermia therapies such as radiofrequency ablation or high-intensity focused ultrasound. To overcome these challenges, the MNPs should be accurately delivered only to the target tumors, the temperature of which can be easily controlled by adjusting the MNP concentration delivered and the proper manipulation of the magnetic field strength. Furthermore, some thermally responsive agents that aid in specific nanoparticle retention within the tumor can reduce the diffusion of MNPs to healthy tissues adjacent to the tumor (Le Renard PE et al., 2010). One of the advantages of magnetic hyperthermia over other clinical hyperthermic treatments is that one is able to repeat the treatment in a short interval without additional invasive procedures. MR scans can predict the distribution of the MNPs to prevent unwanted heating of the normal tissues. If the nanoparticles accurately cover the tumor tissues on a short-term follow-up MR, magnetic hyperthermia is able to be repeated without causing major side effects. Furthermore, local overheating may be avoided by selecting particles with a low maximal achievable temperature while preserving the magnetization for efficient heating (Krishnan S et al., 2010). Among the many MNPs, Resovist is clinically approved for contrast-enhanced MR in human (Reimer P and Balzer T, 2003) and was previously reported to generate effective heat in

AMF (Takamatsu S et al., 2008). Choosing an MNP already approved for clinical use was our main strategy to facilitate early translation of our study into clinical practice.

The tumor cells in the center of the tumor tissues are not sensitive to chemotherapy due to hypoxia but are sensitive to hyperthermia due to low pH value, whereas the tumor cells in the tumor periphery are sensitive to chemotherapy (de Smet M et al., 2013, Sun X et al, 2010). Hyperthermia, when it is applied to specific lesions, produces increased perfusion to the diseased area and makes the cells more permeable for better cellular uptake of agents. Therefore, when the hyperthermia is combined with chemotherapy for cancer, the heat that is generated in the targeted tumor can induce higher levels of drug accumulation in the tumor cells by the same mechanism described above. Doxorubicin is visualized by fluorescence microscopy with excitation wavelength at 480 nm (Karukstis KK et al, 1998), which enables us to detect the doxorubicin deposits in the tumor tissues. In our study, the fluorescence intensity was much higher in group D than in group B, suggesting an increased and long-lasting uptake of doxorubicin into the cells in group D (Fig. 9).

Although doxorubicin has been widely used as single agent or in combination with other anticancer drugs for HCC (Zhu AX, 2006), the drug

produces many side effects derived from its nonspecific uptake into healthy normal tissues (Kang YM et al., 2011). Therefore, recent studies have focused on the development of administration routes for doxorubicin to increase tissue selectivity (Al-Abd AM et al., 2010). Local administration of the agent is one promising approach with the advantage of reaching high concentrations at the target site more effectively than systemic delivery (Kim YI and Chung JW, 2008). Although we injected the therapeutic agents directly into the tumor by the naked eye in our study, we are designing a future project to create an orthotopic liver tumor in which we can inject the therapeutic agents under image guidance using ultrasonography. Our future experiment using an orthotopic model is expected to provide more translatable data.

In this study, we performed BLI for in vivo monitoring of the therapeutic effect. BLI requires a reporter construct produce luciferase, an enzyme that provides imaging contrast by light emission resulting from luciferase-catalyzed conversion of D-luciferin to oxyluciferin in small animals (Zinn KR et al., 2008). Our data demonstrated that the tumor activity signals in group D were significantly lower than those in groups B and C at the end of follow-up period (Fig. 6). Fourteen days after treatment, the BLI signal intensity reverted to 31% of the baseline value in group D, whereas those of groups B and C reverted to 90% and 113%, respectively. Although hyperthermia

applied in the absence of doxorubicin exhibited a marked reduction in the BLI signal in the early stages of treatment, the signal was fully recovered at day 14 post-treatment. However, combination therapy using the Resovist/doxorubicin complex demonstrated a BLI signal that did not rebound during the 14 days post-treatment, representing persistent antitumor efficacy.

In conclusion, the biomedical application of nanomaterials is gradually increasing and is a challenging area for future research. Despite the a significant progress with respect to MNP platforms, regulatory approval for use in humans requires extensive safety studies of newly developed particles. To overcome challenges for clinical translation, we proposed an innovative approach that exploits MNPs conjugated with an anti-cancer drug to achieve efficient drug release and thermotherapy in a single platform composed of agents already approved for use in humans. Our study has several limitations. First, due to the power of the magnetic induction field and the duration of heating, we did not examine the influence of the method on other organs in vivo. Second, we did not investigate the circulation of Resovist/doxorubicin complex particles in the blood. Despite these limitations, we determined that combination therapy using the Resovist/doxorubicin complex could enhance anti-tumor efficacy in an HCC model by simultaneous induction of hyperthermia and drug delivery. This system enables a multi-modal therapy

that can provide an efficient strategy against cancer based on both physical (heat) and chemical (drug) properties. We hope that our results will help to facilitate the clinical translation of MNPs for their future development.

Reference

Al-Abd AM, Hong KY, Song SC, Kuh HJ. (2010) Pharmacokinetics of doxorubicin after intratumoral injection using a thermosensitive hydrogel in tumor-bearing mice. J Control Release. 142, 101-107.

Cole AJ, Yang VC. David AE. (2011) Cancer theranostics: the rise of targeted magnetic nanoparticles Trends in Biotechnology. Trends Biotechnol. 29, 323-332.

de Smet M, Hijnen NM, Langereis S et al. (2013) Magnetic resonance guided high-intensity focused ultrasound mediated hyperthermia improves the intratumoral distribution of temperature-sensitive liposomal doxorubicin. Invest Radiol. 48, 395-405.

El-Serag HB, Rudolph L. (2007) Hepatocellular carcinoma : epidemiology and molecular carcinogenesis. Gastroenterology. 132, 2557-2576.

Facy O, Radais F, Ladoire S, et al. (2011) Comparison of hyperthermia and adrenaline to enhance the intratumoral accumulation of cisplatin in

a murine model of peritoneal carcinomatosis. J Exp Clin Cancer Res. 30:4.

Hegyi G, Szigeti GP, Szász A. (2013) Hyperthermia versus Oncothermia: Cellular Effects in Complementary Cancer Therapy. Evid Based Complement Alternat Med. 2013, 12.

Hilger I, Hergt R, Kaiser WA. (2000) Effects of magnetic thermal ablation in muscle tissue using iron oxide particles. An in vitro study. Invest Radiol. 35, 170-179.

Hong S, Leroueil PR, Janus et al. (2006) Interaction of polycationic polymers with supported lipid bilayers and cells: nanoscale hole formation and enhanced membrane permeability. Bioconjug Chem. 17, 728-734.

Ito A, Tanaka K, Honda H et al. (2003) Complete regression of mouse mammary carcinoma with a size greater than 15 mm by frequent repeated hyperthermia using magnetite nanoparticles. J Biosci Bioeng. 96, 364-369.

Jordan A, Wust P, Fahling H et al. (2009) Inductive heating of ferrimagnetic

particles and magnetic fluids; physical evaluation of their potential for hyperthermia. Int J Hyperthermia 25, 499-511.

Kang YM, Kim GH, Kim JI et al. (2011) In vivo efficacy of an intratumorally injected in situ-forming doxorubicin/poly(ethylene glycol)-b-polycaprolactone diblock copolymer. Biomaterials. 32, 4556-4564.

Karukstis KK, Thompson EH, Whiles JA, Rosenfeld RJ. (1998) Deciphering the fluorescence signature of daunomycin and doxorubicin. Biophys Chem. 73, 249-263.

Kelsey L, Tinkum, Luciano Marpegan et al. (2011) Bioluminescence Imaging Capture the Expression and Dynamics of Endogenous p21 Promoter Activity in Living Mice and Intact Cells. Molcular and Cellular Biology. 31(18), 3759-3772.

Kim YI, Chung JW. (2008) Selective or targeted gene/drug delivery for liver tumors: advantages and current status of local delivery. Expert Rev Gastroenterol Hepatol. 2, 791-802.

Krishnan S, Diagaradjane P, Cho SH. (2010) Nanoparticle-mediated thermal therapy: evolving strategies for prostate cancer therapy. Int J Hyperthermia. 26, 775-789.

Li SD, Huang L. (2009) Surface modification of nanoparticles evading the reticuloendothelial system: Role of the supported bilayer. Biochem Biophys Acta. 1788, 2259-2266.

Le Renard PE, Jordan O, Faes A et al. (2010) The in vivo performance of magnetic particle-loaded injectable, in situ gelling, carriers for the delivery of local hyperthermia. Biomaterial. 31, 691–705.

Purushotham S, Ramanujan RV. (2010) Thermoresponsive magnetic composite nanomaterials for multimodal cancer therapy. Acta Biomater. 6, 502–510.

Reimer P, Balzer T. (2003) Ferucarbotran (Resovist): a new clinically approved RES-specific contrast agent for contrast-enhanced MRI of the liver: properties, clinical development, and applications. Eur Radiol 13, 1266-1276.

Schwartz M, Roayaie S, Konstadoulakis M. (2007) Strategies for the management of hepatocellular carcinoma. Nat Clin Pract Oncol. 4, 424-432.

Sun X, Xing L, Ling CC, Li GC. (2010) The effect of mild temperature hyperthermia on tumour hypoxia and blood perfusion: relevance for radiotherapy, vascular targeting and imaging. Int J Hyperthermia. 26, 224-231.

Takamatsu S, Matsui O, Gabata T et al. (2008) Selective induction hyperthermia following transcatheter arterial embolization with a mixture of nano-sized magnetic particles (ferucarbotran) and embolic materials: feasibility study in rabbits. Radiat Med. 26, 179-187.

Thiesen B, Jordan A (2008) Clinical applications of magnetic nanoparticles for hyperthermia. Int J Hyperthermia. 24, 467–474.

Veiseh O, Gunn JW, Zhang M. (2010) Design and fabrication of magnetic nanoparticles for targeted drug delivery and imaging. Adv Drug Deliv Rev. 62, 284–304.

Wahajuddin, Arora S. (2012) Superparamagnetic iron oxide nanoparticles:

magnetic nanoplatforms as drug carriers. Int J Nanomedicine. 7, 3445-3471.

Weissleder R, Elzonde G, Wittenberg J et al. (1990) Ultrasmall superparamagnetic iron oxide: characterization of a new class of contrast agents for MR imaging. Radiology. 175, 489–493.

Wust P, Gneveckow U, Johannsen M et al. (2006) Magnetic nanoparticles for interstitial thermotherapy--feasibility, tolerance and achieved temperatures. Int J Hyperthermia 22, 673-685.

Zhu AX. (2006) Systemic therapy of advanced hepatocellular carcinoma: how hopeful should we be? Oncologist. 11, 790-800.

Zinn KR, Chaudhuri TR, Szafran AA et al. (2008) Noninvasive bioluminescence imaging in small animals. ILAR J. 49, 103-115.

국문초록

최근 들어 암을 수술하지 않고 병변 부위에 국소적으로 열을 발생시켜 암을 치료하는 고주파열치료(RFA; Radio Frequency Ablation)와 고강도집속초음파치료(HIFU; High Intensity Focused Ultrasound) 열치료법 들이 많이 개발되며 현재 임상에서 활발하게 사용하고 있다. 그러나 RFA의 경우 시술 자체가 침습적이고 발생하는 열이 100℃에 육박하는 아주 높은 온도라서 환자에게 심한 통증을 주고, 각종 부작용과 합병증의 발생 빈도가 10% 정도로 보고되고 있으며, 합병증 발생시 치명적인 경우가 많아 시술 관련 mortality rate가 1% 정도 된다(Ann Surg. 2004 April; 239(4): 459-463)고 알려져 있다.

Mild temperature hyperthermia에 의한 암 치료는 기본적으로 암세포가 정상세포보다 열에 더 민감하다는 가설에 기반하고 있으며 thermal ablation method이 50℃ 이상의 고열에 의해 암세포를 coagulation시켜 죽이는데 반해(indirect effect), hyperthermia에서는 40~45℃ 의 열에 의해서도 정상 세포의 생리 작용은 비활성화되고(Curr. Med. Chem. 2010;17:3045), hyperthermia가 항암면역기전을 활성화시켜 치료 효과를 증진시킨다는(indirect effect) 연구들이 보고되고 (Immunol Res 2010;26:137)있다.

따라서 우리는 이 부분에 초점을 맞추어 자성나노입자를 이용한 mild temperature hyperthermia(MTH)에 관해 알아보았다.

자성나노입자는 AMF(Alternating magnetic field)에 반응하여 Neel and Brownian relaxation의 따른 magnetic moment의 oscillation에 의해 열이 발생한다는 장점과 표면을 약물로 코팅 처리하게 되어 약물전달체로 활용할 수 있다는 장점을 가지고 있다. 이러한 장점을 이용하여 임상적으로 승인된 Iron oxide particle인 MRI Liver contrast agent (Ferucarbotran: Resovist)에 항암제(doxorubicin)을 붙여 Resovist-doxorubicin complex 를 만들었다.

다음과 같이 4그룹(Group A : Control, Group B : doxorubicin group, Group C : Resovist group, Group D : Resovist-doxorubicin group)의 항암동물모델을 이용하여 항암제 탑재 자성나노입자의 항암열화학치료 시너지 효과에 관해 알아보았다.

각 그룹내 개체의 종양 활성도를 BLI (Bioluminescence imaging) 촬영하며 모니터링을 진행하였으며 종료일인 14일 후 3그룹(Group A : Control, Group B : doxorubicin group, Group C : Resovist group)의 BLI signal intensity 가 증가하는 반해 항암제 탑재 자성나노입자군(Group D : Resovist-doxorubicin group)에서의 BLI의 Relative Signal Intensity(RSI)가 현저히 감소하는 것을 알 수 있

었다. 더불어, 병리조직 검사(H&E: Hematoxylin and eosin staining, TUNEL: Terminal deoxynucleotidyl transferase-mediated nick end labeling)를 통해 항암제탑재 자성나노입자를 이용한 항암열화학치료가 항암 효과를 항진 하는것으로 확인 하였다. 자성나노입자에 탑재한 독소루비신 항암제가 470nm파장대에서 형광을 가진다는 장점을 이용하여 실험 종료 후 종양조직 내 남아있는 약물을 형광현미경으로 확인시 항암제 탑재 자성나노입자군(Group D)에서 더 많은 형광을 띄는 것으로 보아 종양 내 약물이 더 많이 잔존하는 것으로 확인하였다.

결과적으로 종양 내 온도가 올라가며 주변의 혈류와 혈관 및 세포막의 permeability를 증가시켜 항암제 탑재 자성나노입자내 항암제가 종양내로 약물의 진입을 용이하게 만들어 항암효과를 항진시킬 뿐아니라, 종양주변의 림프혈관시스템이 잘 발달되어있지 않으므로 암조직으로 주입된 입자가 배출되지 않고 오랫동안 오래 머무르는 EPR(Enhanced Permeability and Retention) 효과가 증가한 것으로 보인다. 더불어, 종양세포 바깥쪽은 약물에 민감하고 내부는 열에 민감하기에 hyperthermia에의해 DNA-repair enzyme을 비활성화 시키며, drug resistance를 감소시켜 전체적으로 항암제의 효과를 항진 시킨 것으로 보인다.

결론적으로, 항암제 탑재 자성나노입자를 종양내에 전달하여,

AMF(Alternating Magnetic Field)에 의해 유도되는 열을 발생시켜 열치료를 함과 동시에, 발생한 열에 의해서 항암제 전달 효과(DDS: Drug delivery system)를 항진시키는 것으로 밝혔다.

주요어 : 자성나노입자, 항암열화학치료, Magnetic hyperthermia, DDS(Drug delivery system), Bioluminescence imaging(BLI)
학 번 : 2012-23674